Tanzania Journal of Engineering and Technology 2025, **44(1)**:72-84
OPEN ACCESS articles distributed under Creative Commons Attribution Licence [CC BY-ND]
Websites: https://ajol.org/tjet; https://tjet.udsm.ac.tz

ISSN 1821-536X (**print**); ISSN 2619-8789 (**electronic**)
https://doi.org/10.52339/tjet.v44i1.981

Regular Research Manuscript

Flood Inundation Mapping for the Tana River Delta in Kenya

Anne N. Mugatha, Patrick Valimba, and Joel Nobert

Department of Water Resources Engineering, University of Dar es Salaam
Corresponding author: mugathaann@gmail.com, ORCID: 0009-0005-3756-2423

ABSTRACT

This study aimed at mapping flood inundation areas in the Tana River Delta. The 30 m DEM and digitized streams and road networks data were collected through remote sensing techniques followed by ground truthing. The data used also included Tana River discharge data at Garsen gauging station. Probability distributions were fitted on the annual maximum discharges. The 4 parameter generalized Gamma probability distribution was the best-fitting distribution according to goodness-of-fit criteria and the Q-Q plots and was used to generate the flood quantiles for different return periods. The generated flood quantiles were; 286 m^3/s, 369 m^3/s, 400 m^3/s, 405 m^3/s, 439 m^3/s, and 449 m^3/s for 2-year, 5-year, 10-year, 20-year 50-year, and 100-year return periods respectively. GIS Flood Tool in ArcGIS used flood quantiles to produce flood extents and inundation depths. The largest part of the Tana River delta was predicted to be flooded with inundation depths of upto 1.8 m causing inundation of settlements and leading to the death of people and livestock, as well as the destruction of properties and infrastructure including roads and buildings, farms, crops, among others. The study established that 31% of the schools located along the Tana River in the Garsen sub-catchment are exposed to inundation depths above 0.5 m. Different flood management options were identified for Tana River Delta and were subjected to Multicriteria Analysis for a decision to be arrived at in choosing the best. Advanced technology in recession agriculture, early warning systems, and forecasting were ranked as the optimal options for managing floods in Tana River Delta. The outcomes of this study contribute to preparedness for floods and guide development decisions within the mapped areas.

ARTICLE INFO

Submitted: Feb. 17, 2024

Revised: Oct. 20, 2024

Accepted: Mar. 17, 2025

Published: Apr. 2025

Keywords: *Climate, Discharge, Flood inundation, Flood quantiles, GIS Flood Tool, Tana River Delta.*

INTRODUCTION

Globally, natural disasters have resulted in billions of dollars' worth of destruction and losses as well as the loss of hundreds of thousands of lives worldwide. One of the most recurring, widespread, disastrous, and frequent natural hazards in the world is flooding, which is a constant threat to life and property (Okoko, 2022). Over the past 30 years, floods have been the most severe natural disaster, impacting, on average, about 80 million people per year (Uddin *et al.*, 2013).

Floods in Africa have a significant negative effect on the populace and their daily lives, causing a great deal of death and economic loss (Di Baldassarre et al., 2010; Tramblay *et al.*, 2020). In Kenya, floods due to too much rainfall have resulted in disasters (Opere, 2013). They have led to a severe loss of life (human and livestock), destruction of property, interference with communication systems, and significant economic losses, degradation of land among others. Amongst the frequently flooded areas in Kenya are those located in lower areas of the Tana River Basin (TRB) within the Tana River Delta (TRD) extending to the Indian Ocean coast.

River Tana is the largest river in Kenya serving a wide range of economic and developmental operations within the food-water-energy nexus as well as different kinds of ecological biodiversity (Omengo *et al*., 2016). The Masinga Reservoir and three more hydropower plants were built to capture floodwater headwaters from the Tana River's primary upper catchment areas where also an inter-basin water transfer scheme exists. Throughout the Tana Delta, farming is predominantly around small towns and villages. Rapid population expansion in the delta communities results in the growth and intensification of farmland by converting natural vegetal land cover to cropland. Increasing conversions and intensification of rainfall amounts have exposed some parts of the Tana River Basin to recurring floods. According to Reliefweb reports (ReliefWeb 2018, 2019, 2021), the Tana River Delta experienced fluvial and flash floods that caused extensive damage to life and properties in the years 2018, 2019, and 2021. The floods experienced in the TRD correspond to overbank flows (Dhar & Nandargi, 2003) particularly in delta floodplains where there are a number of distributaries. This study therefore aimed at flood inundation mapping in the delta.

MATERIALS AND METHODS

Description of the Study Area

Located wholly within Kenya, the Tana River Basin is bordered by the Ewaso Ng'iro, Rift Valley, and Athi basins to the north, west, and south, respectively. Its headwaters are on Mount Kenya and the Aberdare Ranges (considered one of Kenya's five water towers) (Tanui *et. al*., 2018). It has a total catchment area of 94700 km^2 (Min. of Water Development, 1978) (Hughes, 1984). It covers 17% of the country's land area. The topography of the basin varies from the uplands of Mount Kenya to the lowlands of Garsen towards the coastline of the Indian Ocean (Figure 1). It has upper, middle, and lower catchments that support the livelihoods of some 6.5 million people, the majority of whom (5.3 million) live in the upper 17,000 km^2 of the basin (TNC 2015). The Tana River Delta (TRD) is located in the lower catchment wholly within the Garsen sub-catchment, (Figure 1). It is in the North of the Indian Ocean coastline, between Garsen, Lamu, and Malindi towns, and extends roughly over 1300 km^2 (Leauthaud *et al*.,2013). The TRD is home to over 100,000 inhabitants (Kenya Population Census, 2009), mostly from the Pokomo, Orma, Somali, Wardei, and Wata communities. The delta provides a whole range of natural resources for the local communities that mainly rely on agricultural production, fishing, and livestock keeping (Leauthaud *et al*., 2012). The soils of the Tana River Delta are developed on recent alluvial deposits from the river. The main soil types encountered are deep, well-drained, dark brown, and cracking 5 vertisols and fluvisols (Kenya Soil Survey,1984a, b). Here and there, small island-like shaped sand dunes form slightly higher grounds where woodlands and forests are established. The clayey nature of the TRD soils probably limits the infiltration of water in the floodplains during inundation events once the soil is swollen and the cracks are reduced (Leauthaud *et al*., 2012). The climate of the basin varies enormously, from 1000 mm of rainfall in the upper catchment (Hughes, 1984), 300 mm in the middle catchment (Garissa), and 600 mm downstream on the coast (Garsen) (Hughes, 1990).

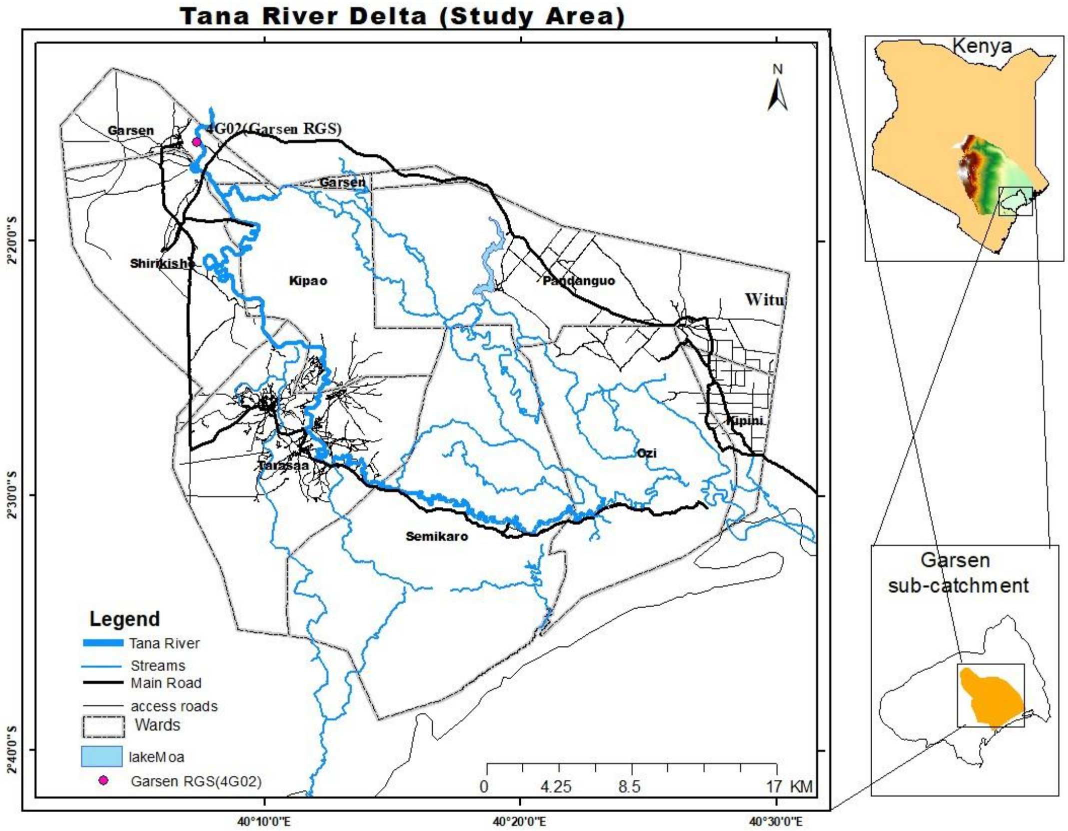

Figure 1: Tana River Delta, rivers, roads, and gauging station.

Data and Data Quality

The streamflow data for Tana River was obtained from Garsen river gauging station (4G02) located at latitude 2°16′6″S, longitude 40°07′35″E, and elevation 17 m (Figure 3.1). The available data in record for the Tana River at Garsen gauging station was for the period 1950-2015. The data was obtained from the Water Resources Authority (WRA) Office in Kenya. After obtaining the data, different data quality control measures were done to ensure that the data used was of good quality. Data validation was done by checking its consistency and format. Data cleaning followed whereby the missing values were filled through linear interpolation and the date formatting issues were corrected. The topography of the study area was represented by the USGS SRTM 30 m resolution Digital Elevation Model (DEM). The DEM was filled using ArcGIS algorithms that find and fill any depression or sinks in the DEM. Digital layers of streams, road networks and the schools' locations data were obtained from Google Earth Pro 2014 and 2018 image. Data for schools and villages in the TRD were obtained from the Ministry of Education and Tana River County profile respectively, and their locations verified on the Google Earth Pro.

Approach

ArcGIS software and GIS Flood Tool model (an extension added to ArcGIS) was used to prepare, process, analyze and model the input data. Generally, this study involved use of two data types namely spatial data and time series data. Data processing was crucial to be able to effectively use the data in the model. The approach to the study involved obtaining the data and imputing it in the ArcGIS and GFT for processing and analysis. Google earth Pro played a crucial role in verifying the geographical locations for the schools and towns within the TRD. The schools and towns data were then overlaid to the resulting inundation maps to analyze the exposure magnitude. To select the optimal flood management option for the TRD, multicriteria analysis (MCA) was conducted. The study was guided by the conceptual framework in Figure 2.

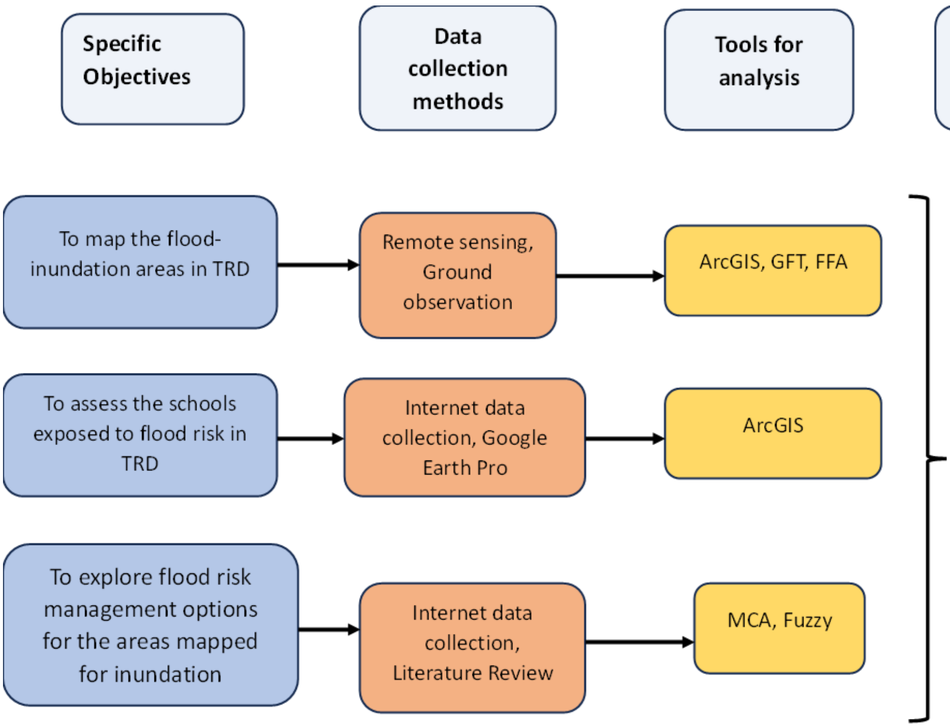

Figure 2: Conceptual framework for the study approach.

Methods

Flood Quantile Estimation

Flood frequency analysis (FFA) was done to obtain different flood quantiles. The Easyfit software was utilized to fit annual maximum discharges at the Garsen gauging station to several probability density functions (pdf). The procedure involved opening the file containing the data onto the calculation window, selecting fit distribution and continuous distributions in a computation window and pressing ok to initiate computation. Evaluation of fitting efficiency involved i) visual analysis of fitted pdf curves plotted on same axes as relative frequency histograms, ii) statistical analysis using goodness-of-fit criteria of Kolmogorov and Smirnov (K-S), Anderson and Darling (A-D) and Chi-Squared (χ^2) (see Table 1 for equations), and iii) the Q-Q plots analysis. The statistical criteria were used in selecting the best 5 pdf and Q-Q plots in selecting fitting discharge ranges for different return periods (the quantiles).

Table 1: Goodness-of-fit criteria (Mert *et al.*, 2015), (Marsaglia, 2004)

Statistic	Definition
Chi-squared	$\chi^2 = \sum_{i=1}^{k} \frac{(O_i - E_i)^2}{E_i}$
K-S	D = max(F(Y_i) – (i-1)/N, i/N – F(Y_i))
A-D	$AD = -n - \frac{1}{n}\sum_{i=1}^{n}(2i-1)[\ln F(X_i) + \ln(1 - F(X_{n-i+1}))]$

Flood inundation mapping

The GIS Flood Tool (GFT) (Kalyanapu *et al.*, 2014; Smith et al., 2018) which is integrated into ArcGIS was used to conduct hydrological modeling to produce flood inundation maps (Figure 2). The GFT tool built a depth-discharge relationship using the Manning's equation (equation (i)). GFT then used the depth-discharge relationship to translate the discharge into the corresponding water depth in the river. The corresponding inundated area was then determined using the Relative DEM. The Relative DEM is a version of the processed input DEM to yield elevation values that are expressed as height above the river. Relative DEM is created in the GFT by using GIS algorithms that condition and process the DEM to allow the definition of the interconnectivity among the pixels (by defining which pixels flow to which). The GFT use of the Manning's equation assumes that, for a given discharge, the surface water depth is uniform along each stream reach (Esri, 2014). The model was therefore calibrated by adjusting the Manning's roughness for the river bed, and different flood quantiles. The Manning's equation is written as;

$$v = \frac{1}{n} R^{\frac{2}{3}} \sqrt{s} \quad \text{equation (i)}$$

where; V is the mean velocity of the cross-section, in meters per second; R is the hydraulic radius, in meters (the cross-sectional area divided by the wetted perimeter); S is the slope of the energy line, dimensionless; and n is the coefficient of roughness ("Manning n"), dimensionless.

To create the hydrologic derivatives needed for the flood hazard mapping using the GFT, the "Hydrology" toolset within the "ArcToolbox" ("Spatial Analyst Tools", "Hydrology") in the ArcGIS was used where several tools were run on the raw DEM.

- Fill: To remove any remaining spurious sinks in the DEM, the "Fill" function was run. This created a depressionless DEM that was used for flow routing and inundation modeling.
- Flow Direction: The depressionless DEM was used to create flow directions.
- Flow Accumulation: The flow direction grid was used to create flow accumulations, which is a grid containing a count of the number of pixels upstream of any location in the DEM. It is often used as a surrogate for flow paths, which is how it was used within the GFT.

The GFT toolbar in ArcGIS has different functionalities that operate stepwise to produce the inundation maps.

Table 2: Sample values of Manning's n (Shaw, E. 2005)

Channel Description	Manning's
Concrete lined	0.013
Unlined earth	0.020
Straight, stable deep channel	0.030
Winding natural stream	0.035
Variable rivers, vegetated banks	0.040
Mountainous streams, rocky beds	0.050

Assessment of the schools exposed to flood risk

In order to do assessment of the schools within the flood inundated areas, data for schools within TRD was collected from the Ministry of Education (MoE) and the Tana River County profile. The geographical locations for these schools were verified through Google Earth pro. Then the schools' data was overlaid to the flood inundation depth maps in the Arc GIS. Analysis was done by assessing the schools' magnitude of exposure to floods.

Exploration of flood risk management options for the TRD

Multicriteria Analysis (MCA) was used to determine the optimum flood management options for the TRD.

- For the different flood management options, this study used cost-effectiveness, and social acceptance as the criteria for choosing the best.
- The conversion scale was employed in the Fuzzy Multi-attribute Decision Making (MADM) theory to translate linguistic scales into fuzzy numbers which range from 0 to 1 in order to

create a decision matrix with precise figures.

- To be able to compare all alternatives, normalization of the decision matrix was done. During normalization, all attributes were converted to an equal scale between 0 and 1.

In this study, normalization was done using the proportional linear transformation equations below;

$$y_{ij}^* = \frac{y_{ij}}{y_{j\max}} \quad \text{for maximization} \quad (1)$$

$$y_{ij}^* = 1 - \frac{y_{ij}}{y_{j\max}} \quad \text{for minimization} \quad (2)$$

y_{ij}^* - Normalized value for *i*-th alternative and *j*-th attribute

y_{ij} – Original value for *i*-th alternative and *j*-th attribute

y_{ij}max – Maximum value for *j*-th attribute

- Weights were assigned to each alternative. The total outcome (V_i) for each alternative was calculated as weighted sum of its respective attribute outcomes (Panjaitan, 2019).

$$V_i = \sum_{j=1} w_j r_{ij} \quad (3)$$

where: V_i is the ranking for each alternative, W_j is the weighted value of each criterion; r_{ij} is the normalized performance rating value.

Each alternative was then ranked in relation to others using a relative scale.

RESULTS AND DISCUSSION

Flood quantiles

The results of the three goodness-of-fit criteria of Kolmogorov-Smirnov (K-S), Anderson and Darling (A-D), and Chi-Squared (χ^2) are shown in Table III. The three goodness-of-fit criteria identified the generalized Gamma 4P, Beta, and Johnson SB as the highest-ranking probability distributions (Table III). The selection of the best distribution among these four used a total rank calculated as the sum of the ranks of the distribution in each criterion. The one with the least total rank was the best-fitting probability distribution. Moreover, the quantile-quantile (Q-Q) plot for each of the three highest-ranking distributions was examined to establish the ranges of quantiles that each distribution fits best. The procedure, therefore, indicated that the 4 parameters generalized Gamma distribution was the best and was used for flood quantile estimation (Table IV). The highest discharge of 447 m^3/s in the 65-year record exceeds the 50-year quantile and is slightly below the 100-year flood.

Table 3: Results of the best fitting probability distributions for annual maximum series at Garsen

Probability distribution	Kolmogorov-Smirnov	Anderson-Darling	Chi-squared	Total	Final Rank
Generalized Gamma 4p	1	2	2	5	1
Beta	2	19	10	31	3
Johnson SB	4	1	7	12	2

Table 4: Flood quantiles for River Tana at Garsen river gauging station

Return period (T), years	2	5	10	20	50	100
Quantile (m^3/s)	286	369	400	405	439	449

Flood inundation maps

Inundation maps were generated for flood quantiles with return periods between 2 years and 100 years. Figure 4 shows the flood inundation depth extent for the different return periods. This could be attributed to the flat topography of the area extending to the Indian Ocean coastal line.

The inundation spread within the area of approximately 1,562 km^2 in the Garsen sub-catchment that is occupied by distributaries of River Tana. The inundated area covers 21.9% of the Garsen sub-catchment. A study conducted by Kiringu, (2015) also indicated the same flood extent in the TRD for a 50 year and 100 year flood quantile with a slight variation for a 2 year flood quantile. The largest part of the inundated area is between the Tarasaa-Pandanguo line to the Indian Ocean coastline. The area south-east of Garsen, east of Minjila, north of Tarasaa town, and west of Kipao, is covered by flood water depth of 1.8 m (Figure 3). Many settlements in Semikaro Ward are in areas exposed to flood water depth of 0.5 m and above. The part located south of lake Moa lies in a flood water depth between 0.5 m to 0.8 m.

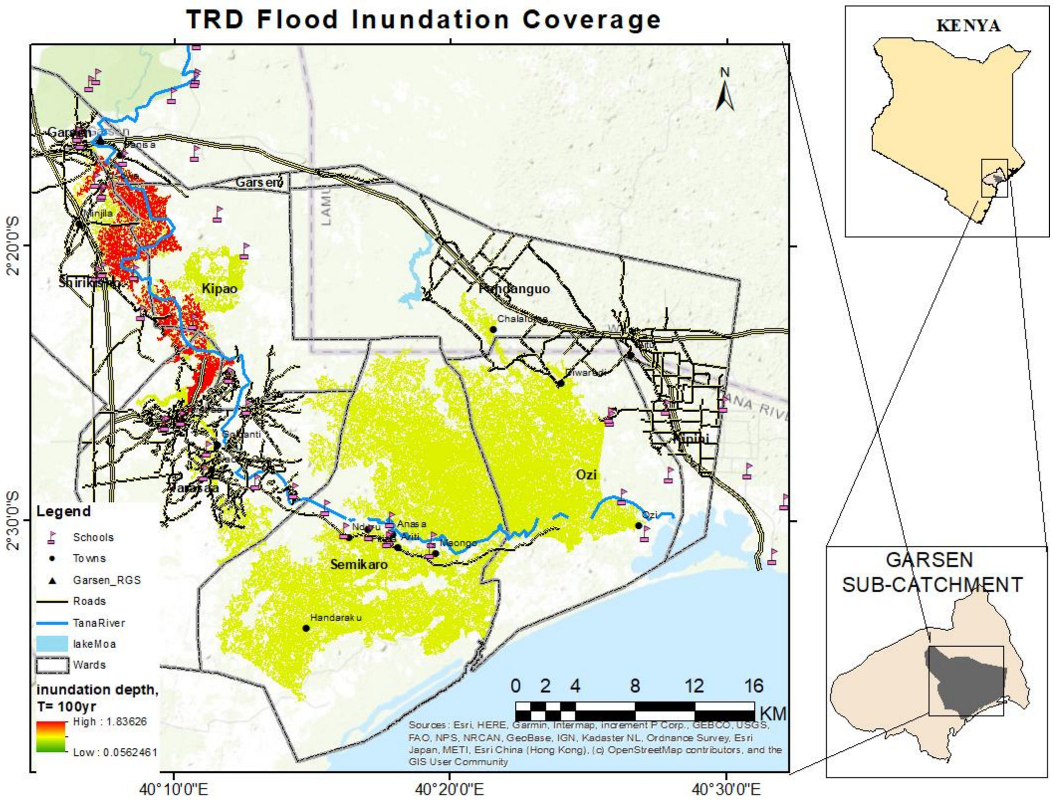

Figure 3: Roads, schools, settlement clusters and 100-year inundation extent.

The rapidly growing populations in these settlements are causing rapid expansion of social services in a way to locate many of them in areas of floodplain where frequent inundation is predicted. Within the Tana River Delta (Lower Tana Basin), floods of 1997/1998, 2007/2008, 2013 (Kiringu 2015), 2018 (reliefweb 2018; Floodlist, 2018; Business Daily News, 2021), 2019 (The Standard Newspaper, 2019; Kenya News Agency, 2019; Floodlist, 2019, Reliefweb, 2019) and 2021 (Reliefweb, 2021) have caused major displacement of people and large economic losses. The economic losses were reflected from infrastructural damages including damages to serving roads, homes and schools, health care facilities in towns and village centers as well as damages to crops in farms and deaths of livestock within the inundated floodplain in the delta.

There are main and access roads connecting settlements, households and facilities within the delta. The main roads are in the periphery of the inundated area except the Garsen-Malindi at the Tarasaa-Ozi road which passes through a 0.5 m to 0.8 m inundated area. The main Garsen-Lamu through Witu tarmac road is mainly aligned outside the periodically inundated floodplain except for a small road section near Witu where a 0.5 m flood inundation is predicted to occur. The Witu road section was affected by the 2021 floods (The Star Newspaper, 2021) despite being predicted to slightly being affected by 0.5 m or less flood inundation (Figure 3). The network of access roads within the towns of Garsen and Witu lies outside the inundated area and therefore are less prone to flooding. The Tarasaa-Ozi road is predominantly passing through an area predicted for flood inundation in the Tarasaa-Ozi section. Floodlist (2019) showed effects of floods since the onset of the short rains in October 2019. It indicated that many roads in Tana River County were blocked and damaged by the flood water. The Standard Newspaper (2019) reported overflown roads by flood water in Mwanja, Handaraku, and Maongo villages in Garsen sub-county, to the extent of forcing villagers to use canoes for movements.

There are around 13 settlements along the Tarasaa-Ozi road section predicted to experience inundation of at least 0.5 m deep as they are all located within the periodically inundated floodplain (Figure 3). In April, 2018, the Business Daily Newspaper reported that these villages were submerged in flood water. The settlements have numerous activities ranging from agriculture, residences, and many social services including academic (schools) and health care facilities (dispensaries, health centers).

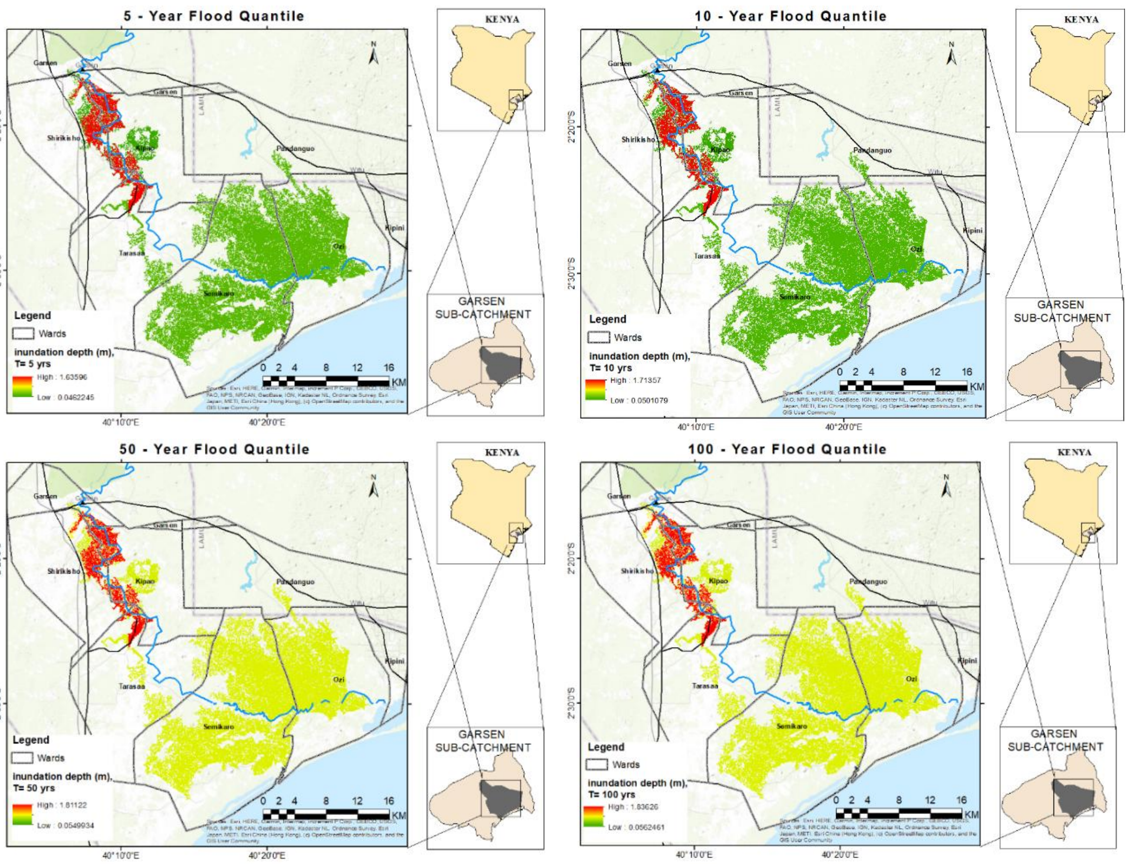

Figure 4: Inundation extent for different flood quantiles.

Assessment of the schools exposed to flood risk

Due to the many socio-economic and settlement activities in Garsen, there are many schools in the area (Figure 3). 58 schools are located along the Tana River in Garsen sub catchment, of which 31% are exposed to the risk of flooding. Of the exposed schools, 34% are in 0.5 m to 1 m flood depth area, and 66% are exposed to floods above 1 m depth. There are 9 primary and secondary schools, which have been affected by floods in 2019 and 2020 damaging classrooms, latrines and access roads (Reliefweb, 2021). The schools, for example, were among the affected properties during the December 2019 floods to the extent that students of Buyani Secondary School were forced to sit for their end-of-year exams at Arap Moi Primary school in Ngao Village due to inundation of the access roads (Kenya News Agency, 2019). The Standard (2018) reported that Ozi and Odole primary schools were partially destroyed by floods. A 0.5 m to 1.8 m flood depth for schools (Figure 3) indicates a substantial and potentially dangerous inundation that has significant implications to the safety, education, and well-being of students, staff, and the entire exposed community as described below:

- The safety of students and staff is exposed to risk. This flood depth poses a serious risk of drowning, particularly for younger children who may be unable to navigate through such deep water.
- Roads (Figure 3) get inundated making schools inaccessible.
- There is need for evacuation to ensure the safety of students and staff.
- Disruptions in education, as schools need to remain closed until floodwaters recede and the area becomes safe again.
- Floodwaters at this depth can cause extensive damage to school buildings, furniture, and equipment. The water can weaken structures and lead to structural failures, making the school buildings unsafe for use even after the floodwaters have receded.
- The structural damages may require significant time and resources to repair, affecting the overall functioning of the schools.
- The floodwaters often carry contaminants, including sewage and debris, which is likely to cause waterborne diseases and pose health risks.
- Experiencing a flood can be traumatic for students, staff, and the community, and the fear and stress caused by the disaster can have lasting psychological effects, particularly on children.
- Families may lose their homes, livelihoods, and possessions during the flood, affecting their ability to support their children's education.

Optimal Flood Management Measures for TRD

Despite the use of several reactive, anticipatory and proactive measures (Raadgever, T., & Hegger, D 2018) against floods to lessen or eliminate impacts of floods to people in TRD, people and properties in the delta have continuously been affected by floods. The different potential measures to reduce the impacts of floods on lives, agricultural farms and infrastructure in TRD were evaluated to identify their suitability in TRD. Multi Criteria Analysis (MCA) (Sabbaghian *et al.,* 2016) was used to identify the most optimal flood management practices for TRD. Six (6) different alternatives identified as:

i) Relocation of houses and important buildings to higher grounds
ii) Use of improved cultivation technology in recession agriculture
iii) Limiting the number of livestock in the inundated areas and moving them to higher grounds during floods
iv) Improving early warning systems and its communicated messages
v) Elevating school grounds and proper designing of infrastructure
vi) Improving enabling environment

The alternatives were analyzed based on two criteria namely social acceptance and cost (Table V). The social acceptance of each alternative was either low, medium, or high, and the cost of implementing each alternative was given in USD (Table V). A conversion scale was employed in the

Fuzzy Multi-attribute decision-making (MADM) theory (Zhang, 2004) to translate the social acceptance linguistic scales into fuzzy numbers to create a decision matrix with precise figures (Table V). The highest fuzzy number indicated the highest social acceptance while the lowest fuzzy number indicated the lowest social acceptance.

Since the two attributes used in this study to select the best flood management option are in different scales of measurement, normalization of the decision matrix was done to convert them to an equal scale to be able to compare them. The proportional linear transformation equations for maximization (equation 3.4-4) and minimization (equation 3.4-5) were used to do normalization. During normalization, all attributes were converted to an equal scale between 0 and 1 (Table VI).

Table 5: Flood management options for TRD and decision matrix (Fuzzy numbers)

Alternatives	Attribute	Criteria		
		Social Acceptance		Cost million $ (USD)
		Level	Fuzzy number	
A1	Relocation of houses and important buildings to higher grounds	Low	0.2	20
A2	Advanced Technology in Recession Agriculture	High	0.8	5
A3	Limiting the number of livestock in the inundated areas and moving them to higher grounds during floods	Medium	0.5	5
A4	Early warning systems and forecasting	High	0.8	5
A5	Elevation of school grounds and proper designing of infrastructure	High	0.8	10
A6	Enabling environment	Medium	0.5	5

Table 6: Normalization of decision matrix

Alternatives	Attribute	Social Acceptance	Cost
A1	Relocation of houses and important buildings to higher grounds	0.25	0
A2	Advanced technology in Recession Agriculture	1	0.75
A3	Limiting the number of livestock in the inundated areas and moving them to higher grounds during floods	0.625	0.75
A4	Early warning systems and forecasting	1	0.75
A5	Elevation of school grounds and proper designing of infrastructure	1	0.5
A6	Enabling environment	0.625	0.75
		maximization	minimization

For each alternative, a weight was assigned for each attribute. The total outcome for each alternative was calculated as weighted sum of its respective attribute outcomes. Alternative with the highest weight value was ranked number 1 (Table VII) indicating that it is the best flood management option for TRD. Therefore, Advanced Technology in recession agriculture and early warning systems and forecasting are the optimal options to manage the floods in TRD.

Table 7: Alternatives Ranked

Alternatives	Attribute	Social Acceptance	Cost	Weight	Rank
A1	Relocation of houses and important buildings to higher grounds	0.25	0	0.1	4
A2	Advanced Technology in Recession Agriculture	1	0.75	0.9	1
A3	Limiting the number of livestock in the inundated areas and moving them to higher grounds during floods	0.625	0.75	0.7	3
A4	Early warning systems and forecasting	1	0.75	0.9	1
A5	Elevation of school grounds and proper designing of infrastructure	1	0.5	0.8	2
A6	Enabling environment	0.625	0.75	0.7	3

CONCLUSION

Flood frequency analysis methods were used on annual maximum discharges of Tana River at the Garsen gauging station. The 4-parameter generalized Gamma probability distribution was the best fitting distribution according to goodness-of-fit criteria and the Q-Q plots and was used to generate the flood quantiles for different return periods. The flood quantiles were used in the GIS Flood Tool to produce flood extents and inundation depths. The study provided a detailed visualization of potential flood scenarios in the TRD. It predicted largest part of the Tana River delta to be flooded with inundation depths of at least 0.5 m causing inundation of settlements as well as destruction of infrastructure including roads, schools, health facilities, farms, crops, and livestock. The study indicated that 31% of the schools located along the Tana River in the Garsen sub-catchment are exposed to inundation of above 0.5 m.

There are 6 flood management options that were identified as the different flood management alternatives for TRD and were subjected to MCA for a decision to be arrived at in choosing the best. The advanced technology in recession agriculture and early warning systems and forecasting were ranked the optimal options for managing floods in TRD.

This study will not only aid in risk assessment but also contribute significantly to informed decision-making for effective flood management and guide development planning. This is also an invaluable asset for developing early warning systems and formulating evacuation strategies.

REFERENCES

Business Daily (2021) KenGen won't pay Garsen flood victims, 29th July 2021. Available online at https://www.businessdailyafrica.com/bd/news/counties/kengen-won-t-pay-garsen-flood-victims--3490740. Retrieved on 9th September 2023.

Dhar, O. N., & Nandargi, S. (2003). Hydrometeorological aspects of floods in India. *Natural Hazards*, **28**, 1-33. doi: 10.1023/A:1021199714487

Di Baldassarre, G., Schumann, G., Bates, P. D., Freer, J. E., & Beven, K. J. (2010). Flood-plain mapping: a critical discussion of deterministic and probabilistic approaches. *Hydrological Sciences Journal–Journal des Sciences Hydrologiques*, **55**(3), 364-376. doi: 10.1080/02626661003683389

Douglas, I., Alam, K., Maghenda, M., Mcdonnell, Y., McLean, L., & Campbell, J. (2008). Unjust waters: climate change, flooding and the urban poor in Africa. *Environment and urbanization*, **20**(1), 187-205. doi: 10.1177/0956247808089156

Esri, 2014, ArcMap 10.2: Redlands, Calif., Esri.

Floodlist (2019) Kenya – Over 100 Dead, 18,000 Displaced After Recent Floods and Landslides, 29th November 2019. Available online at https://floodlist.com/africa/kenya-floods-november-2019. Retrieved on 9th September 2023.

Frankhauser, S., & Schmidt-Traub, G. (2011). From Adaptation to Climate resilient Development: The cost of Climate-proofing the MDGs in Africa. *Clim. Dev*, **3**(20), 94-113. doi: 10.1080/17565529.2011.582267

Hughes, F. M. (1984). A comment on the impact of development schemes on the floodplain forests of the Tana River of Kenya. *Geographical Journal*, 230-244. doi: 10.2307/635001

Hughes, F. M. (1990). The influence of flooding regimes on forest distribution and composition in the Tana River floodplain, Kenya. *Journal of Applied Ecology*, 475-491. doi: 10.2307/2404295

Kalyanapu, A. J., Ghafoor, S. K., Marshall, R. J., Dullo, T. T., Judi, D. R., & Shankar, S. (2014). Benchmark Exercise for Comparing the Computational Performance of Two-Dimensional Flood Models in CPU, Multi-CPU, and GPU Frameworks. *In World Environmental and Water Resources Congress* 2014 (pp. 1322-1331). doi: 10.1061/9780784413548.133

Kenya News Agency (2019) Over 200 Flood Victims Of 2018 Benefited From Free Modern Housing Project In Garsen, 13th November 2019. Available online at https://www.kenyanews.go.ke/over-200-flood-victims-of-2018-benefited-from-free-modern-housing-project-in-garsen/. Retrieved on 9th September 2023.

Kenya News Agency (2019) Over 3,000 People in Garsen Are Marooned Following The Bursting Of River Handarakulagha, 19th November 2019. Available online at https://www.kenyanews.go.ke/over-3000-people-in-garsen-are-marooned-following-the-bursting-of-river-handarakulagha/. Retrieved on 9th September 2023.

Kiringu, K. (2015). Consideration of factors that affect flood levels in the Tana River Delta in Kenya (Doctoral dissertation, Stellenbosch: Stellenbosch University). http://hdl.handle.net/10019.1/96890

Leauthaud, C., Belaud, G., Duvail, S., Moussa, R., Grünberger, O., & Albergel, J. (2013). Characterizing floods in the poorly gauged wetlands of the Tana River Delta, Kenya, using a water balance model and satellite data. *Hydrology and Earth System Sciences*, **17**(8), 3059-3075. doi: 3059-3075. 10.5194/hess-17-3059-2013

Leauthaud, C., Duvail, S., Belaud, G., Moussa, R., Grünberger, O., & Albergel, J. (2012). Floods and wetlands: combining a water-balance model and remote-sensing techniques to characterize hydrological processes of ecological importance in the Tana River Delta (Kenya). *Hydrology and Earth System Sciences Discussions*, **9**(10), 11267-11318. doi: 10.5194/hessd-9-11267-2012

Okoko, A. N. (2022). The legacy of vulnerability to floods in the Tana River, Kenya. International *Journal of Disaster Risk Reduction*, 71, 102833. doi: 10.1016/j.ijdrr.2022.102833

Omengo, F. O., Geeraert, N., Bouillon, S., & Govers, G. (2016). Deposition and fate of organic carbon in floodplains along a tropical semiarid lowland river (Tana River, Kenya). *Journal of Geophysical Research: Biogeosciences*, **121**(4), 1131-1143. doi: 10.1002/2015JG003288

Opere, A. (2013). Floods in Kenya. In *Developments in earth surface processes* (Vol. 16, pp. 315–330). Elsevier. DOI: 10.1016/B978-0-444-59559-1.00021-9.

Panjaitan, M. I. (2019). Simple Additive Weighting (SAW) method in determining beneficiaries of foundation benefits. *Login*, **13**(1), 19–25 doi: 10.24224/login.v13i1.22

Raadgever, G. T. (Tom), Booister, N., & Steenstra, M. K. (2018). Integrated Planning, Coordination and Collaboration. In T. Raadgever & D. Hegger (Eds.), *Flood Risk Management*

Strategies and Governance (pp. 109–123). Springer International Publishing. doi:10.1007/978-3-319-67699-9_10

Reliefweb (2018) At least 70 schools fail to re-open in flood-hit Tana River, 2nd May 2018. Available online at https://reliefweb.int/report/kenya/least-70-schools-fail-re-open-flood-hit-tana-river. Retrieved on 9th September 2023.

Reliefweb (2019) UNICEF sends supplies to flood-affected children and families in 12 counties in Kenya, 4th December 2019. Available online at https://reliefweb.int/report/kenya/unicef-sends-supplies-flood-affected-children-and-families-12-counties-kenya. Retrieved on 11th September 2023.

Reliefweb (2021) Kenya: Floods - Apr 2021. Available online at https://reliefweb.int/disaster/fl-2021-000038-ken. Retrieved on 11th September 2023.

Sabbaghian, R. J., Zarghami, M., Nejadhashemi, A. P., Sharifi, M. B., Herman, M. R., & Daneshvar, F. (2016). Application of risk-based multiple criteria decision analysis for selection of the best agricultural scenario for effective watershed management. *Journal of Environmental Management*, **168**, 260-272. doi: 10.1016/j.jenvman.2015.11.038

Shaw, E. (2005). *Hydrology in practice*. CRC press. https://api.taylorfrancis.com/content/books/mono/download?identifierName=doi&identifierValue=10.1201/9781482268386&type=googlepdf

Tanui, J., & Saina, C. K. (2015). The physical state of forest cover and land use in Kenya-a case of nandi hills forests in Nandi County, Kenya. *European-American Journals*.

The Star Newspaper (2021). Homes along Lamu-Garsen road flooded over poor drainage, 18th June 2021. Available online at https://www.the-star.co.ke/counties/coast/2021-06-18-homes-along-lamu-garsen-road-flooded-over-poor-drainage/. Retrieved on 9th September 2023.

The Standard (2018) Schools fail to reopen as rains persist, 3rd May 2018. Available online at https://www.standardmedia.co.ke/health/health-science/article/2001279028/schools-fail-to-reopen-as-rains-persist. Retrieved on 11th September 2023.

The Standard Newspaper (2021). Flooding menace wreaks havoc in Garsen over Christmas season, 30th December 2019. Available online at https://www.standardmedia.co.ke/sports/north-eastern/2001354742/www.digger.co.ke. Retrieved on 9th September 2023.

Tramblay, Y., Villarini, G., & Zhang, W. (2020). Observed changes in flood hazard in Africa. *Environmental Research Letters*, **15**(10), 1040b5. doi: 10.1088/1748-9326/abb90b

Uddin, K., Gurung, D. R., Giriraj, A., & Shrestha, B. (2013). Application of remote sensing and GIS for flood hazard management: a case study from Sindh Province, Pakistan. *American Journal of Geographic Information System*, **2**(1), 1-5. doi: 10.5923/j.ajgis.20130201.01

Verdin, J., Verdin, K., Mathis, M. L., Magadzire, T., Kabuchanga, E., Woodbury, M., & Gadain, H. (2016). A software tool for rapid flood inundation mapping. In *Open-File Report* (Nos. 2016–1038). U.S. Geological Survey. doi: 10.3133/ofr20161038

Zhang, W. (2004). Handover decision using fuzzy MADM in heterogeneous networks. *2004 IEEE Wireless Communications and Networking Conference* (IEEE Cat. No. 04TH8733). doi: 10.1109/WCNC.2004.1311263